PERGAMON

International Journal of Solids and Structures 39 (2002) 3337–3357

INTERNATIONAL JOURNAL OF SOLIDS and STRUCTURES

www.elsevier.com/locate/ijsolstr

Instability, shear banding, and failure in granular materials

Poul V. Lade *

Department of Civil Engineering, Aalborg University, Sohngaardsholmsvej 57, 9000 Aalborg, Denmark

Received 13 February 2002

Abstract

Two modes of decrease in load bearing capacity of granular materials are discussed in view of experimental results. Both relate to the fact that frictional materials exhibit nonassociated plastic flow and they undergo considerable volume changes, either contraction or dilation. One mode consists of the instability that may occur in certain regions of stress space and potentially result in liquefaction of the granular material. It is the fact that loading of contracting soil (resulting in large plastic strains) can occur under decreasing stresses that may lead to unstable behavior under undrained conditions. As long as the soil remains drained, it will remain stable in the region of potential instability. The other mode is initiated by localization of plastic strains and subsequent development of shear bands, which in granular materials is followed by a decrease in load bearing capacity. These two modes are mutually exclusive and they occur for different loading and material conditions as discussed here on the basis of experimental observations.

Keywords: Contraction; Dilation; Failure; Granular materials; Instability; Liquefaction; Nonassociated flow; Shear banding

1. Introduction

Several modes of decrease in load bearing capacity, often referred to as failure, have been identified from experiments on granular materials. The strength of granular materials is primarily proportional with the effective confining pressure, and the load bearing capacity therefore decreases with decreasing confining pressure. Reduction in effective confining pressure may be caused by increasing pore pressure and will result in failure. Another well-known mode is the smooth peak failure occurring at constant confining pressure in which the internal structure of the granular material is loaded and deformed sufficiently to cause collapse of load bearing chains of particles. The resulting reduction in load bearing capacity is characterized as material softening, and it involves macroscopically uniform deformations and stresses such that the granular material can be characterized as a continuum.

Two additional modes of decrease in load bearing capacity have been observed. Both relate to the fact that frictional materials exhibit nonassociated plastic flow and they undergo considerable volume changes, either contraction or dilation. One mode consists of the instability that may occur in certain regions of

* Fax: +45-98-142555.
E-mail address: lade@civil.auc.dk (P.V. Lade).

0020-7683/02/$ - see front matter
PII: S0020-7683(02)00157-9

stress space and potentially result in the well-known phenomenon referred to as liquefaction. Another mode is initiated by localization of plastic strains and subsequent development of shear bands, which in granular materials is followed by a decrease in load bearing capacity. These latter two modes are mutually exclusive and they occur for different loading and material conditions as discussed here on the basis of experimental observations.

Results of previously performed series of triaxial compression tests designed to expose the type of behavior displayed by granular materials have shown that materials that exhibit nonassociated flow do not obey the stability postulates by Drucker and Hill. Triaxial tests on fully saturated and partly saturated specimens of sand have been performed under drained and undrained conditions to study the regions of stable and unstable behavior. Granular materials may become unstable *inside* the failure surface if the state of stress is located between the instability line and the failure surface for the material. Thus, instability is not synonymous with failure, although both may lead to catastrophic events such as gross collapse of earth structures. Conventional slope stability methods do not capture the mechanics of instability and subsequent liquefaction that may occur in gently inclined submarine slopes, in tailings dams, and in earth and snow avalanches. It is the fact that loading of a contracting soil (resulting in large plastic strains) can occur under decreasing stresses that leads to unstable behavior under undrained conditions. Loose, fine sands and silts have sufficiently low hydraulic conductivities that small disturbances in load or even small amounts of volumetric creep may temporarily produce undrained conditions in such soils, and instability of the soil mass follows. As long as the soil remains drained, it will remain stable in the region of potential instability.

The occurrence of shear banding in the plastic hardening regime limits the strength of the soil. Shear banding occurs in the softening regime in conventional triaxial compression tests. However, true triaxial tests have been performed to study the effect of shear banding on failure in the full range of the intermediate principal stress. The experiments show that the strength increases as $b = (\sigma_2 - \sigma_3)/(\sigma_1 - \sigma_3)$ increases from 0 to about 0.18, then remains almost constant until b reaches 0.85, and then decreases slightly at $b = 1.0$. Shear banding initiates in the hardening regime for b-values of 0.18–0.85. Thus, peak failure is caused by shear banding in this middle range of b-values, and a smooth, continuous three-dimensional failure surface is therefore not obtained in general for soils. Analysis based on theoretical conditions and experimental results agree on the occurrence of shear banding and its consequent effect on the three-dimensional failure conditions for soil.

2. Instability

Experimental evidence from tests on several types of soils have clearly indicated that the use of conventional associated flow rules in formulation of elasto-plastic constitutive models results in prediction of too large volumetric expansion. To characterize the volume change correctly, it is necessary to employ a nonassociated flow rule. The plastic potential surfaces do therefore not coincide with the yield surfaces, but the two families of surfaces cross each other.

The application of nonassociated flow rules for soil have resulted in questions regarding uniqueness and stability of such materials. The stability postulate for time-independent materials due to Drucker (1951, 1956, 1959) is satisfied provided that associated plastic flow is employed in construction of constitutive models involving convex, plastic yield surfaces. Hill's stability condition (Bishop and Hill, 1951; Hill, 1958) is expressed in terms of total strain increments (elastic and plastic), and it extends the condition for stability a little beyond that due to Drucker. Theoretical considerations have suggested that they are not necessary conditions (Mroz, 1963; Mandel, 1964).

Experiments to study whether or not granular materials are unstable under certain load conditions have been performed. In these studies instability was taken to be the inability of the material to sustain or carry a given load. This includes the inability to sustain small perturbations in the load. Several series of triaxial

compression tests designed and performed to expose the type of behavior displayed by granular materials are reviewed. The results of these experiments show that a positive value of the second increment of plastic work is neither a necessary nor a sufficient condition for stability of granular (frictional) materials. Experimental observations of stability and instability are reported, and stability conditions for materials with nonassociated flow are presented.

2.1. Stability postulates

Stability as formulated by Drucker (1951, 1956, 1959) contains two elements as expressed by plastic work increments:

$$\mathrm{d}W_{\mathrm{p}} - \mathrm{d}W_{\mathrm{p}}^{*} = (\sigma_{ij} - \sigma_{ij}^{*})\dot{\varepsilon}_{ij}^{\mathrm{p}} \geqslant 0 \tag{1}$$

$$\mathrm{d}^2 W_{\mathrm{p}} = \dot{\sigma}_{ij}\dot{\varepsilon}_{ij} \geqslant 0 \tag{2}$$

in which σ_{ij} is a stress state on the yield surface, σ_{ij}^{*} is a stress state inside the yield surface, $\dot{\sigma}_{ij}$ is stress increment starting at σ_{ij} causing plastic strain increment $\dot{\varepsilon}_{ij}$.

Eq. (1) is commonly referred to as stability in the large, and it implies that the yield surface must be convex. Eq. (2) is referred to as stability in the small, and it is fulfilled if the plastic strain increment vector is normal to the yield surface. This implies that the plastic potential surface is identical to the yield surface, so that when yielding occurs, the plastic strain increment is normal to the yield surface. Therefore, Drucker's stability postulates imply associated flow rules, and they are applicable for solid metals, which can be reasonably characterized by associated flow rules.

Eq. (2) has often been taken to define stable and unstable behavior. If the condition is satisfied for any stress increment, then the material is unconditionally stable. The material may be conditionally stable, if Eq. (2) is fulfilled for some stress increments and not for others. The material will be completely unstable if Eq. (2) is not satisfied for all possible stress increments. Eq. (2) is always negative for the condition following peak failure, which results in complete instability.

Bishop and Hill (1951) and Hill (1958) extended the condition for stability slightly beyond that proposed by Drucker by expressing it in terms of total strain increments:

$$\mathrm{d}^2 W = \dot{\sigma}_{ij}\dot{\varepsilon}_{ij}^{\mathrm{t}} = \dot{\sigma}_{ij}(\dot{\varepsilon}_{ij}^{\mathrm{e}} + \dot{\varepsilon}_{ij}^{\mathrm{p}}) = \dot{\sigma}_{ij}\dot{\varepsilon}_{ij}^{\mathrm{e}} + \dot{\sigma}_{ij}\dot{\varepsilon}_{ij}^{\mathrm{p}} \geqslant 0 \tag{3}$$

in which $\dot{\varepsilon}_{ij}^{\mathrm{t}}$ is the total strain increment, and $\dot{\varepsilon}_{ij}^{\mathrm{e}}$ is the elastic strain increment.

Stability postulates developed by Drucker, and by Bishop and Hill provide sufficient conditions to ensure stability. However, theoretical considerations by Mroz (1963), Mandel (1964), and Nemat-Nasser (1983) have suggested that they are not necessary considerations for stability.

Experimental evidence for soils has generally indicated that conventional associated flow rules consistently predict too large volumetric dilation, which is indicated by the condition that the plastic strain increment is not normal to the yield surface. Therefore, proper soil constitutive models need incorporate nonassociated flow rules, in which there is a separate plastic potential surface, which is not coincidental with the yield surface.

2.2. Consequences of nonassociated flow

A typical pattern of yield surfaces for an isotropic soil is shown on the triaxial plane in Fig. 1. In three dimensions these yield surfaces are shaped as asymmetric tear drops. For an isotropic material the yield surfaces intersect the hydrostatic axis at right angles, they bend smoothly backwards towards the origin, and they cross the failure surface at sharp angles.

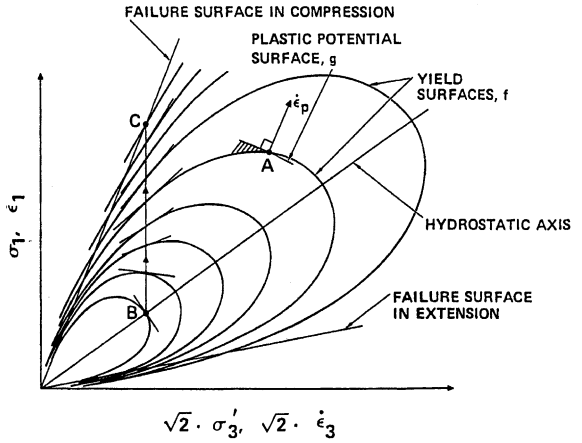

Fig. 1. Pattern of yield surfaces for isotropic soils. Stress path for conventional triaxial compression test (BC).

Plastic potential surfaces for nonassociated flow have similar shapes as yield surfaces, but the two families of surfaces cross each other. Experimental evidence for granular materials indicate that the plastic potential surfaces have more pointed ends and they resemble cigars with asymmetric cross-sections. A typical plastic potential surface is shown at point A in Fig. 1.

The shaded wedge between the yield surface and the plastic potential surface defines a region in which Eq. (2) is not fulfilled, because a stress increment starting at point A and contained in this wedge will produce a negative scalar product. With a negative scalar product Drucker's stability postulate indicates that the material should exhibit unstable behavior. However, drained experiments show that the sand is perfectly stable at stress points where the normal to the yield surface points in the outward direction of the hydrostatic axis. For this condition the deviator stress can be safely increased to produce further plastic shear strains (work-hardening). In other words, the sand can sustain higher loads and behave in an inelastic manner without undergoing any instability or collapse.

Instability may occur when the yield surface opens up in the outward direction of the hydrostatic axis. This allows plastic strains (loading) to occur while the stresses are decreasing. Here loading occurs inside the failure surface and instability may develop in the form of inability to sustain the current deviator stresses.

Fig. 1 shows the stress path for a conventional triaxial compression test performed at constant confining pressure. As the specimen is loaded from B to C the inclination of the yield surface changes. At low deviator stresses near point B, the yield surface is inclined towards the outwards direction of the hydrostatic axis. As loading proceeds, the inclination of the yield surface changes gradually and becomes inclined towards the origin as failure is approached at point C. It is in this region of high deviator stresses where the yield surface is inclined toward the origin that instability may occur. This region is indicated in Fig. 2.

Fig. 2 shows a wedge between the current yield surface f and the plastic potential surface g corresponding to the current stress point. For a dilating material this wedge shaped region is located within a larger region bounded by lines corresponding to $(\sigma_1'/\sigma_3') = \text{const.}$ and $(\sigma_1 - \sigma_3) = \text{const.}$ All stresses, including the stress difference, are decreasing within the wedge between f and g, but the stress ratio (σ_1'/σ_3') is increasing in this region. By performing triaxial tests with stress paths located in this region, experimental evidence regarding the instability of materials with nonassociated flow can be obtained.

It is important to recognize that the material behavior obtained for stress paths within the shaded wedge in Fig. 2 corresponds to work-hardening with positive plastic work, $dW_p > 0$, and outward motion of the

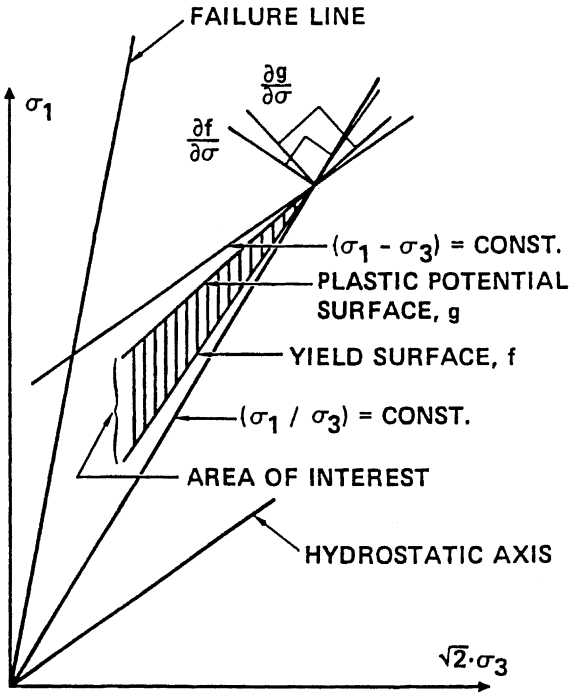

Fig. 2. Wedge-shaped region of stress paths with decreasing stresses in which soils with nonassociated flow may be unstable during hardening inside the failure surface.

yield surface. Although the stresses in any direction within the wedge are decreasing, failure has not been reached and softening of the material is therefore not occurring.

2.3. Stability in drained compression

Several series of triaxial compression tests were performed to study stability and instability in granular materials. The details of these experiments are given by Lade et al. (1987, 1988) and by Lade and Pradel (1990).

To demonstrate that nonassociated plastic flow is obtained for granular materials, the results of a drained triaxial test on fine silica sand are shown in Fig. 3. This test was performed with a stress path inside the failure surface involving primary loading (hardening) with decreasing stress difference $(\sigma_1 - \sigma_3)$ and decreasing confining pressure σ_3. If stresses and strain increments are plotted on the same diagram, as in Fig. 3(b), the direction of the plastic strain increment vector is uniquely determined from the state of stress, and it is independent of the stress path leading to this state of stress as shown by Poorooshasb et al. (1966) and Lade and Duncan (1976). The stress path with decreasing stresses, shown in Fig. 3(b), is so steep as to form an obtuse angle $(\beta - \alpha) = 110°$ with the direction of the plastic strain increment vector. Thus, the condition in Eq. (2) is violated.

The fact that plastic yielding is occurring along the stress path with decreasing stresses is seen from the stress–strain curve in Fig. 3(a). Section BC on the stress path is labeled similarly on the stress–strain curve which indicates large plastic strains between B and C. Since the yield surface is being pushed out, it must be steeper than the stress path direction BC. If it were less steep, so as for example to be perpendicular to the plastic strain increment vector thereby indicating associated flow, then point C would be inside the yield

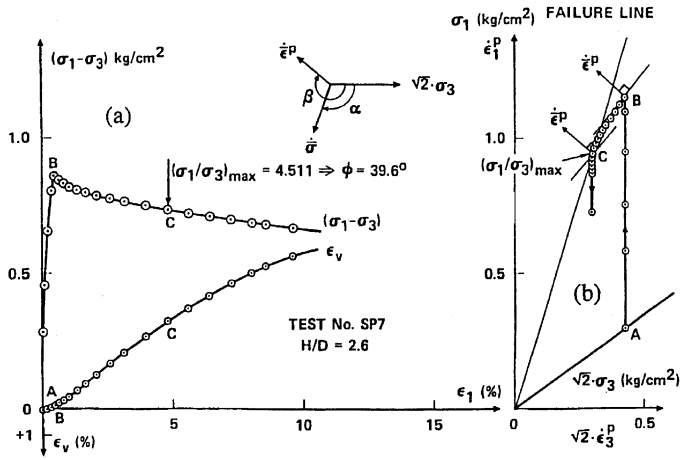

Fig. 3. (a) Stress–strain and volume change curves and (b) stress path and plastic strain increment vectors for test on fine silica sand.

surface passing through point B corresponding to unloading from B to C. This would contradict the large plastic strains shown in Fig. 3(a). Consequently, the yield surface must be steeper than stress path BC, and nonassociated plastic flow is therefore clearly indicated.

In order to expose the potential instabilities in soil behavior that might occur for the stress paths in the prefailure region described earlier (see Fig. 2), it is necessary to perform triaxial tests under stress control. A series of drained tests similar to that shown in Fig. 3 was therefore performed under stress control (Lade et al., 1987). In fact, the test shown in Fig. 3 is one of these tests. Seven experiments were performed. They all exhibited plastic dilation, and they all clearly showed nonassociated flow. When the sand specimens were exposed to stress paths in the region of potential instability, *none was observed*, i.e. run-away instability was not encountered. The tall cylindrical specimens with lubricated ends deformed as perfect right cylinders with no developing shear bands, no bulging or shearing in a nonuniform manner, or any other signs of instability. Little but negligible creep was present in the sand specimens. Thus, stable behavior was observed in the region in which Drucker's stability postulate was violated.

Regardless of the ability to define yield surfaces from experiments, the fact remains that negative values of d^2W_p are obtained from direct experimental measurements. The fact that the specimens remained stable implies that the behavior is not strain softening, i.e. the peak strength has not been exceeded. Therefore, to model this behavior through any type of normality would require a serious departure from plasticity theory.

In order to investigate whether the type of volume change (dilation or contraction) was important for stability of granular soils, a second series of tests was performed on sand that contracted during shear (Lade and Pradel, 1990). Drained tests with stress paths within the shaded wedge shown in Fig. 2 were performed on loose sand that exhibited contraction during shear. Although Drucker's stability condition was violated inside the failure surface, none of the specimens showed any signs of run-away instability.

The results of these two series of triaxial compression tests demonstrated that drained conditions produced stable behavior irrespective of (1) the sign of the second increment of work (2) the sign of the volumetric strain (dilation or contraction), and (3) the sign and direction of the increments in stress components. Thus, under fully controlled conditions such as those prevailing for drained conditions, unstable run-away situations cannot occur. These results therefore clearly show that Drucker's stability postulate is not a necessary condition for stability.

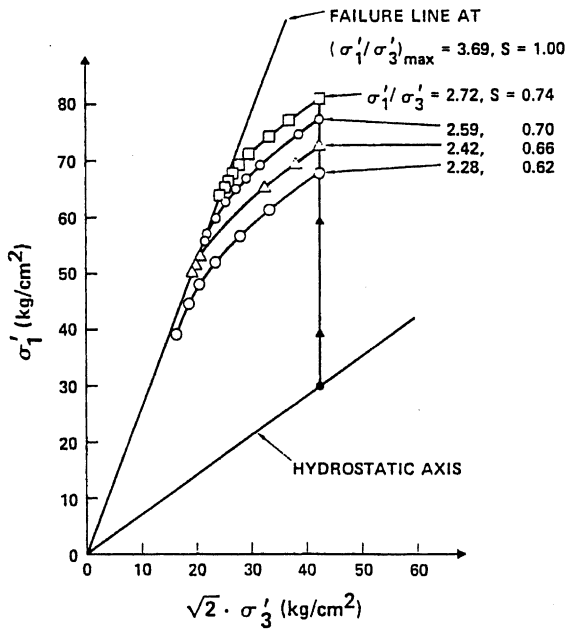

Fig. 4. Effective stress paths for stress-controlled triaxial compression tests on loose Sacramento River sand.

2.4. Instability in undrained compression

On the other hand, fully saturated soils that tend to contract during shear may become unstable *inside* the failure surface and this may lead to liquefaction. A series of stress controlled tests was performed on granular soil that tended to contract during shear (Lade et al., 1988). The specimens were exposed to stress paths within the shaded wedge shown in Fig. 2. Fig. 4 shows the actual stress paths followed in these tests, and Fig. 5 shows the observed stress–strain, volume change, and pore pressure development in one of the tests. In each test the saturated specimen was first loaded under drained conditions to a preselected stress level S (expressed as the ratio of the current to the maximum stress difference at a given confining pressure). The drainage valve was then closed and instability developed in each specimen due to increasing pore pressure, i.e., the specimens could not sustain the applied load. The tendency for volumetric creep, however small it may be, caused the pore pressure to increase under undrained conditions, providing the small perturbation which rendered the material unstable. However, the large strains observed along the unstable stress paths could not be caused by creep or viscous flow as shown by Lade et al. (1988). The effective stress paths shown in Fig. 4 were within the shaded wedge in Fig. 2, the specimens exhibited nonassociated flow and plastic volumetric contraction (although the total volumetric strain was zero), and instability was obtained in all cases in the hardening regime *inside* the failure surface.

In the studies presented here instability was taken to be the inability to sustain or carry a given load, which includes the ability to sustain small perturbations in the loads. However, the possibility that instability might manifest itself as localization of plastic deformation and development of shear planes or in any other way was not overlooked. The specimens were therefore inspected after the tests (they were enclosed in a steel walled triaxial apparatus and could not be observed during the tests) at which time they had sustained 15–30% axial strain. The instabilities were induced at axial strain of 2.8–5.3%. Thus, substantial amounts of strain had occurred after the instabilities were induced. Nevertheless, the specimens

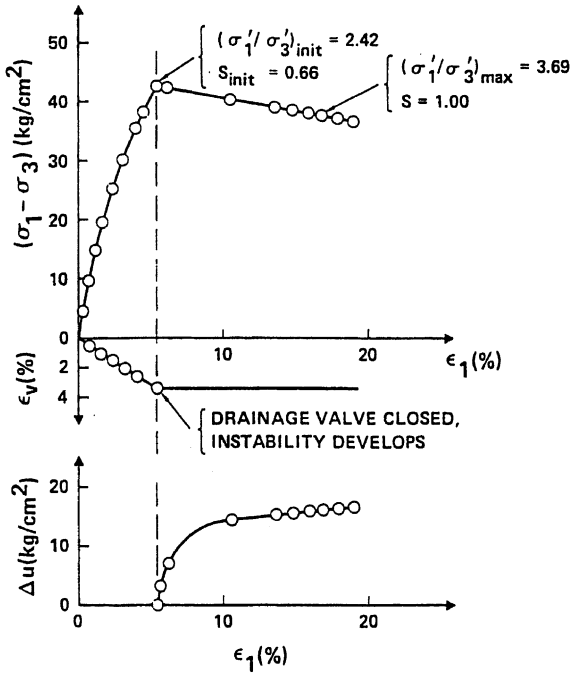

Fig. 5. Stress–strain, volume change, and pore pressure relations in stress-controlled triaxial compression test on loose Sacramento River sand.

had bulged only slightly and there were no visible shear planes. In fact, a uniform distribution of horizontal wrinkles in the membrane was observed after each tests, thus revealing a fairly uniform pattern of internal strains in the specimens. Instability did not appear to be associated with localization of plastic deformations and consequent shear banding of the type discussed by Lade (1982) and Peters et al. (1988). This is consistent with previous observations that shear planes are not observed in soils that contract (Lade, 1982).

2.5. Observations for partly saturated sand

Stress paths with only one particular direction is obtained from undrained tests on fully saturated soils at each particular stress state, as shown in Fig. 4. In order to study the soil behavior for other stress path directions under undrained conditions, a series of tests, similar to those described above, was performed on specimens with decreasing degree of saturation (Lade and Pradel, 1990). By purposely introducing a controlled amount of compressible air into the specimens, the undrained effective stress paths could be pointed in different directions within the shaded wedge in Fig. 2. The specimens in the tests in which the effective stress paths were inside the shaded wedge exhibited unstable behavior. Tests with stress path above the shaded wedge, created by introducing an amount of air in the specimen greater than critical, indicated stable behavior.

The conclusions from the experiments are that sand that tends to contract can become unstable if the degree of saturation is sufficiently high and if the drainage condition is changed from drained to undrained. This may occur in fine sands and silts in which the hydraulic conductivity is relatively low, thus enhancing the undrained condition in the presence of relatively fast loading conditions.

2.6. Instability of dilating sand

In a discussion of the experimental results reported above, Peters (1991) suggested that even dilating sand may become unstable: if a rate of volumetric expansion were imposed on an element of granular material and this rate exceeded the rate of expansion exhibited by the material, then the effective confining pressure would decrease and the element would become unable to sustain the current, applied shear stress. According to the definition, the material element would become unstable. Thus, a rate of volume change (whether positive, zero, or negative) imposed on a material element could cause it to become unstable depending on the rate of volume change exhibited by the soil itself (contraction of dilation). The soil exhibits an inherent rate of volume change at a given point in stress space (as determined from the direction of the plastic strain increment), but small variations in rate of volume changes are associated with the stress path direction. This is because the total volume change consists of plastic and elastic contributions, and the latter is dependent on the stress path direction. Thus, to study this hypothesis experimentally, a series of triaxial compression tests was performed with appropriate test conditions. The results confirm the suggestion that even dilating sand may become unstable (Lade et al., 1993).

Another test was performed differently from the previous experiments. Instead of reducing the effective confining pressure through injection of water and consequent increase in pore pressure, the test was performed in a drained condition and the total confining pressure was reduced. The specimen was unable to hold the load, i.e. it behaved in an unstable manner. Thus, instability of the specimen is conditional on a progressive reduction in effective confining pressure. The similarity between these test results indicates that instability of dilating sand can be produced by decreasing effective confining pressure whether it is caused by increasing pore pressure or decreasing total confining pressure.

2.7. Conditions for stability and instability

The stability of granular materials which exhibit nonassociated flow has been investigated on the basis of experimental observations. Several series of triaxial compression tests designed to expose the type of behavior exhibited by granular materials were performed. The variables in these studies were the sign of the second work increment (positive or negative), the volumetric strain behavior (contraction or dilation), the constraints on the volumetric behavior (free or controlled), and the degree of saturation (fully or partly saturated).

If physical instability is defined as a condition for which the current, applied shear stress cannot be sustained for perturbations in the state of stress, then contractive as well as dilative materials may be considered to be unstable in the region where the yield surface opens up in the outward direction of the hydrostatic axis. In this region, plastic strains can be produced under decreasing stresses. For undrained conditions and contractive material, the instability is self-sustaining and unconditional, i.e. it is not dependent on conditions outside the soil element. For drained conditions, the instability is conditional, i.e. the decrease in load carrying capability depends on the reduction in effective confining pressure. This reduction may occur as a decrease in total confining pressure or as an increase in pore pressure caused by injection of water into the soil element.

Figs. 6 and 7 show schematic diagrams of the conditions for stability and instability of contracting and dilating granular materials. The shear stress is represented by the stress deviator invariant J_2' and the mean normal stress is indicated by the stress invariant I_1. The generic yield surfaces, f, and plastic potential surfaces, g, cross each other at points (A) where the yield surfaces open up in the outward direction of the hydrostatic axis. Stability is obtained when J_2' is constant or increases, whereas instability occurs when J_2' decreases. The signs of the second increment of work d^2W can be negative in the region of stability, whereas d^2W can be positive in the region of instability for dilating material. The stability postulates by Drucker and

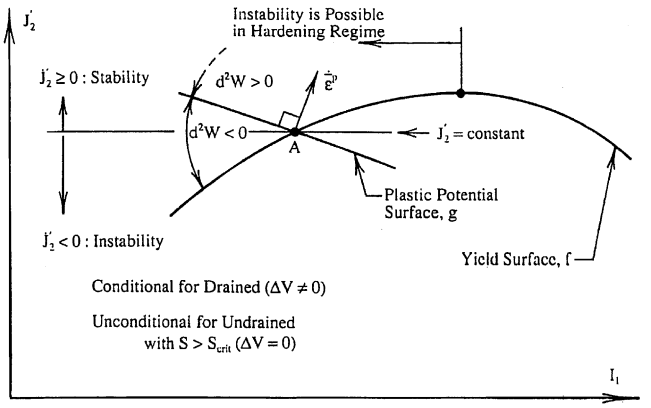

Fig. 6. Schematic diagram of conditions for stability and instability of contracting granular material.

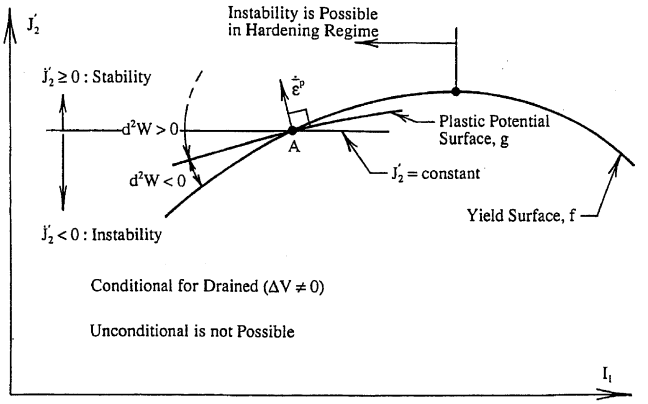

Fig. 7. Schematic diagram of conditions for stability and instability of dilating granular material.

by Hill therefore provide neither necessary nor sufficient conditions for stability of granular (frictional) materials.

2.8. Region of potential instability

It is the fact that loading of a contracting soil (resulting in large plastic strains) can occur under decreasing stresses that leads to unstable behavior under undrained conditions. Loose, fine sands and silts have relatively low hydraulic conductivities, and small disturbances in load or even small amounts of volumetric creep may produce undrained conditions in such soils, and instability of the soil mass follows. As long as the soil remains drained, it will remain stable in the region of potential instability.

When the condition of instability is reached, the soil may not be able to sustain the current stress state. This stress state corresponds to the top of the current yield surfaces as shown schematically on the $p' - q$ diagram in Fig. 8. Following this top point the soil can deform plastically under decreasing stresses. The top of the undrained effective stress path, corresponding to $(\sigma_1 - \sigma_3)_{max}$, occurs slightly after but close to the top of the yield surface. The difference is due to the additional stability provided by the elastic strains, as expressed in Eq. (3).

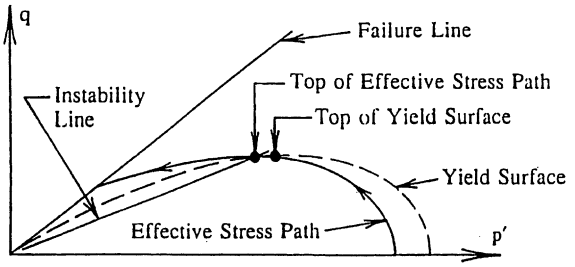

Fig. 8. Location of instability line for loose sand.

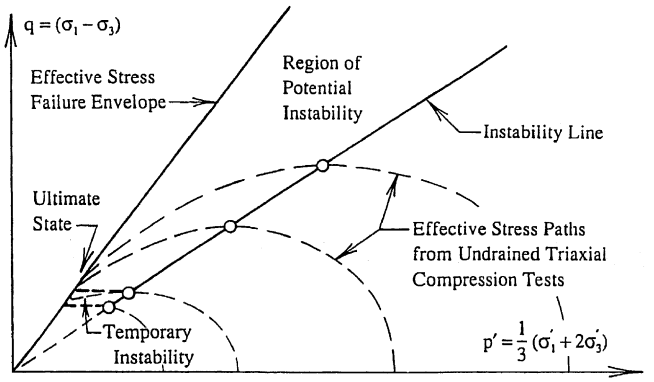

Fig. 9. Schematic diagram of location of instability line in $p' - q$ diagram.

In order for a granular material to become unstable, the state of stress must be located on or above the instability line. Fig. 9 shows a schematic $p' - q$ diagram in which the line connecting the tops of a series of effective stress paths from undrained tests on loose soil provides the lower limit of the region of potential instability. In the region above this instability line the soil can deform plastically under decreasing stresses. Experiments show that this line is straight. Since it goes through the top points of the yield surfaces which evolve from the origin, as shown in Fig. 1, the instability line also intersects the stress origin. Fig. 9 also shows a region of temporary instability which is located in the upper part of the dilating zone. It is a region where instability may initially occur, but conditions allow the soil to dilate after the initial instability, thus causing the soil to become stable again. For very loose soils the region of potential instability reaches down to the origin of the stress diagram.

2.9. Instability versus failure

Instability and failure are two different behavior aspects of soils which exhibit nonassociated flow (Lade, 1989). Although both may lead to catastrophic events, they are not synonymous. However, two criteria for "failure" are commonly used in geotechnical engineering for interpretation of results of triaxial tests on soils: (1) failure occurs when the stress difference reaches a limiting value, $(\sigma_1 - \sigma_3)_{max}$, and (2) failure occurs when the effective principal stress ratio reaches a limiting value, $(\sigma'_1/\sigma'_3)_{max}$. The two conditions are reached simultaneously in drained tests. The confusion as to the definition of failure arises in interpretation of undrained tests on loose sands and sensitive clays in which the pore pressures increase monotonically during shear. For these types of soils the maximum stress difference is reached before the maximum effective

stress ratio. The choice of failure criterion varies with the purpose for which the strength is to be used. Typically, $(\sigma_1 - \sigma_3)_{max}$, is employed in total stress analyses, and $(\sigma'_1/\sigma'_3)_{max}$ is used in effective stress analyses. These issues have been discussed at length by e.g. Bjerrum and Simons (1960), Seed et al. (1960), and Whitman (1960).

Based on the presentation above, it is clear that the condition of maximum stress difference does not correspond to a true failure condition, i.e. it occurs inside the failure surface. Rather, it corresponds to a condition of minimum stress difference at which instability may develop *inside* the true failure surface. Stress states can be reached above the minimum stress difference condition described by $(\sigma_1 - \sigma_3)_{max}$, and instability can be induced anywhere between the $(\sigma_1 - \sigma_3)_{max}$-condition and the true failure surface described by $(\sigma'_1/\sigma'_3)_{max}$. Therefore, a failure condition expressed in terms of the maximum stress difference obtained from e.g. undrained tests initiated at the hydrostatic axis (see Fig. 9) would clearly underestimate the true effective strength of the soil.

Material models which employ associated plastic flow rules must assume the failure surface to go through the point at which instability is produced. This is because stability is guaranteed according to Drucker's and Hill's stability conditions until the failure surface is reached, at which instability ensues. But then stable loading to higher stress differences, which is clearly possible, could not be predicted by such models. Further, since instability as well as stability can be obtained at any point in the region above the line defined by the maximum stress differences in Fig. 9, it is not possible to define any one consistent failure surface to be used in a model which incorporates associated flow.

3. Shear banding

The type of instability discussed above is not the same as that manifesting itself by shear bands. During the performance of the triaxial compression test shown in Fig. 10, the specimen was carefully observed for early detection of developing shear planes. The location on the stress–strain curve at which the first observation of a shear plane was made is indicated on the diagram. Considerable straining beyond the peak failure point may be required before shear bands occur in compression tests. The stress–strain curve clearly shows a drop in strength and the rate of dilation diminishes substantially immediately before the shear plane becomes visible. Thus, the reduced rate of dilation appears to be associated with the occurrence of the shear band and the achievement of critical state conditions within the shear plane in the compression test. Once a shear band has developed fully, the stresses and the volume changes tend to level off, the specimen outside the developing shear band unloads elastically, and the material inside the shear band loosens up to the critical void ratio (Desrues et al., 1996) and rapidly becomes weaker than the remaining major parts of the specimen.

Experimental results with respect to the formation of shear banding under generalized principal stress conditions are available from only few previous studies (e.g. Arthur et al., 1977; Arthur and Dunstan, 1982; Vardoulakis, 1980; Desrues et al., 1985, 1996; Yoshida et al., 1993; Finno et al., 1996, 1997). On the basis of radiographic studies Finno et al. (1996, 1997) pointed to the existence of complex patterns of density fluctuations and early development of strain localizations as precursor to shear banding within plane strain specimens, in which the external deformation apparently continued homogeneously.

Development of shear bands in triaxial compression occurs after peak failure and results in further decrease in strength. This behavior appears to be associated with dilation of the sand. Shear bands are not observed in loose specimens that contract during shear. Loose specimens deform uniformly throughout the entire stress–strain relationship. Fig. 11 shows a critical state diagram for triaxial compression tests on granular materials in which the conditions for stable and unstable behavior as well as for development of shear bands are summarized. Several investigators (Peters et al., 1988, Hettler and Vardoulakis, 1984, Molenkamp, 1985) have shown that the plastic hardening modulus H is required to reach a critical value H_c

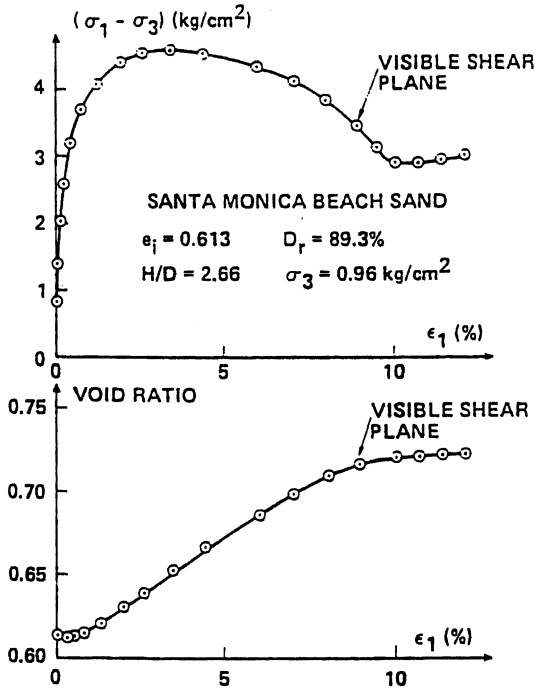

Fig. 10. Stress–strain relation and void ratio change from triaxial compression test exhibiting strain-softening and development of shear plane.

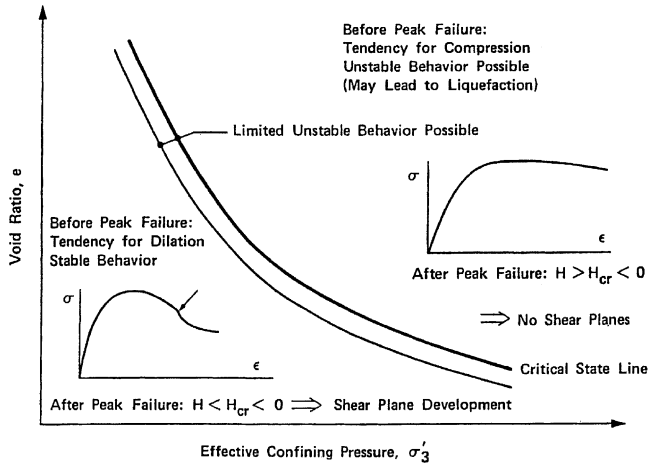

Fig. 11. Critical state diagram for behavior of granular material in triaxial compression. Occurrence of stable and unstable behavior and development of shear planes are indicated.

for development of shear planes. For triaxial compression conditions the critical hardening modulus has to reach a certain negative value before shear planes can develop. This finding is supported by the test results shown in Fig. 10, and it is indicated on Fig. 11.

It appears from these results and from the experimental observations presented above that the type of instability resulting in shear planes is not the same as that discussed in connection with the stability/instability issue presented here. Based on the experimental observations, the two types of instability appear to be mutually exclusive, i.e., shear planes are observed after peak failure in granular materials that dilate, and these materials are perfectly stable for all possible stress path directions before the failure surface has been reached. On the other hand, shear planes are not observed in granular materials that contract during shear, but they can become unstable for certain stress-path directions *inside* the failure surface.

Comparison of stress–strain relations from triaxial and plane strain tests on sand indicates that the three-dimensional stress condition has a significant influence on the formation of shear bands and therefore on the strength of the sand. Peters et al. (1988) found that shear banding can occur in the hardening regime of the stress–strain relationship for sand under plane strain conditions. This experimental finding agrees with the theoretical conclusion by Rudnicki and Rice (1975) for materials with nonassociated plastic flow. On the other hand, shear banding in triaxial compression and extension appears to be a post-peak phenomenon, though it occurs much closer to peak failure in triaxial extension. The fact that peak failure in plane strain tests is associated with the occurrence of shear banding makes it crucial to determine whether failure occurs as a smooth peak or is induced by shear banding over an extended range of intermediate principal stresses.

Experimental studies of shear banding in true triaxial tests have been performed with a modified version of Lade and Duncan's cubical triaxial device (1973). The three-dimensional strength characteristics and the influence of shear banding on failure were studied and the peak strengths are compared with the failure criterion proposed by Lade (1977) and the Mohr–Coulomb failure criterion. Quantitative comparisons are made between the critical conditions for shear band formation obtained from the experiments and from theoretical considerations and expressed by the dimensionless hardening parameter H_c/E immediately prior to the onset of shear banding. Here E is the elastic modulus of the soil.

3.1. Experimental procedures

The cubical triaxial apparatus shown in Fig. 12 and described by Lade and Duncan (1973) was modified for this study. Tests were performed on tall prismatic specimens, 76 mm wide, 76 mm long, and 188 mm high with a height-to-diameter ratio, $H/D = 2.47$ (Wang and Lade, 2001). These tall specimens were employed, because shear bands develop more freely and softening behavior is more pronounced in tall and slender specimens. Extra steel lamellas and balsa wood strips were employed to increase the height of the horizontal loading plates to match the 188 mm tall prismatic specimens. The bars connecting the two horizontal loading plates were still positioned at mid-height, so there was no eccentricity of the horizontal load. Both the horizontal loading plates and the cap and base were provided with lubricated surfaces to avoid development of significant shear stresses between the loading plates and the specimen.

The experiments were conducted on dense, medium dense, and loose Santa Monica Beach sand with void ratios of 0.63, 0.68, and 0.76 corresponding to relative densities of 90%, 74%, and 50%. All specimens were tested with a constant effective confining pressure of $\sigma'_3 = 49$ kPa. Twelve drained tests were conducted with constant b-values from 0 to 1.0 for each relative density.

3.2. Experimental results

3.2.1. Stress–strain characteristics

The stress–strain curves obtained from the true triaxial tests on tall prismatic specimens of dense sand are shown in Fig. 13. The arrows on the stress–strain curves indicate the positions of the peak failure points, and the number indicates the b-value. For $b = 0$ (triaxial compression), the stress–strain curve is essentially flat over a relatively large range of strains near failure, and the slope at failure is zero. Considerable

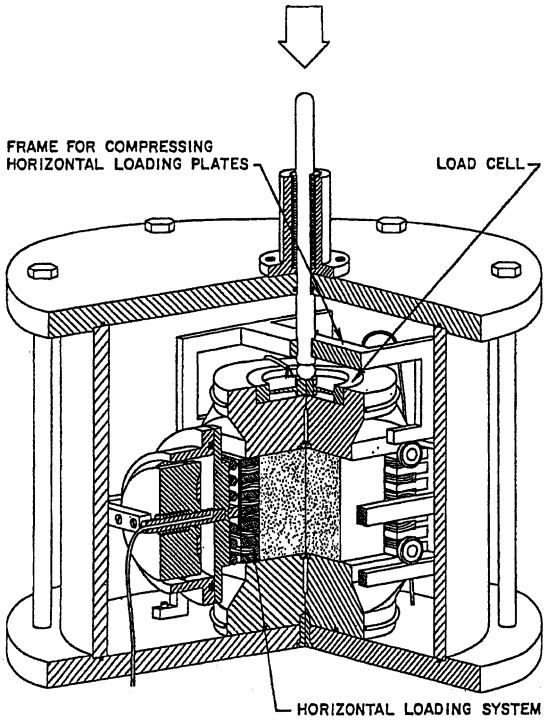

Fig. 12. Cubical triaxial apparatus.

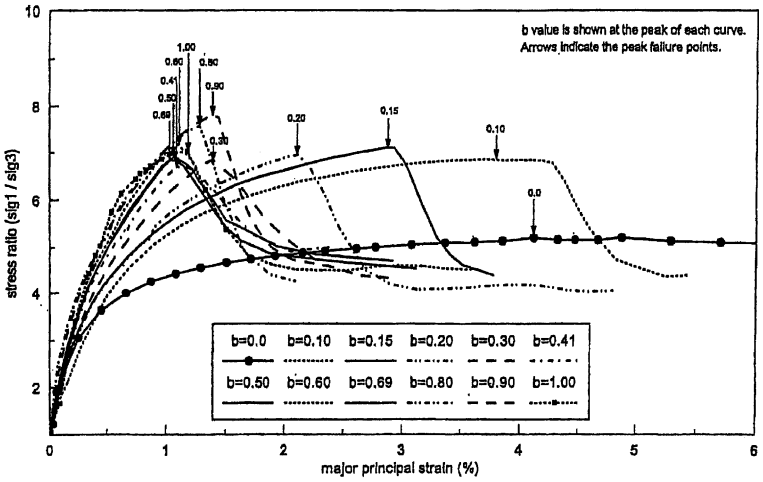

Fig. 13. Comparison of stress ratio–strain characteristics in true triaxial tests on prismatic specimens of dense Santa Monica Beach sand with $\sigma_3' = 49$ kPa.

amounts of softening and strength reduction occurs after failure (not shown in Fig. 13, but indicated in Fig. 10), but shear bands were not observed until a major principal strain of two-and-a-half times the strain-to-peak-failure had been reached.

As b increases from 0 the stress–strain behavior becomes increasingly stiff and the strain-to-failure decreases. The strengths obtained at $b = 0.10$ and 0.15 are considerably higher than that at $b = 0$. The strengths did not drop off after peak failure in these two tests until small amounts of post-peak softening had occurred, as indicated in Fig. 13. After less than 0.5% post-peak straining was obtained, the rate of strength reduction suddenly increased and soon reached its highest value. Shear bands were usually observed when the strength was dropping at the highest rate. After considerable reduction in strength had been obtained, the strength reduction slowed down, the shear bands became well-defined, and the strength reached its residual state.

For the tests performed with b-values in the range of 0.20–0.80, it appears that the strengths drop suddenly at points on the stress–strain curves where the specimens are apparently still being loaded, i.e. the slopes of the curves are positive. There are no smooth peaks on the stress–strain curves obtained in those tests. The peak points appear to represent points of instability occurring before smooth peak failure points can be obtained. Visible shear bands were detected when the strengths were dropping at the highest rates. The residual strengths were reached within 0.7% or less post-peak straining for the tests with b-values in the range of 0.20–0.80.

The peak failure becomes smooth again at $b = 0.90$. However, for the test at $b = 1.00$, the slope of the stress–strain curve prior to failure becomes steeper again and the vertical stress ratio (σ'_1/σ'_3) drops abruptly at the peak. The specimen failed in the horizontal direction at $b = 1.00$, and it was traversed by vertical shear planes parallel to the direction of the major principal stress, whereas vertical failure and shear planes parallel to the intermediate principal stress direction always occurred in the tests with $b = 0$–0.90. Failure occurred in the horizontal load-controlled direction at $b = 1.00$, because the specimens were produced by dry pluviation in the vertical direction, and the consequent cross-anisotropic fabric was weaker in the horizontal than in the vertical direction. The peak point and the post-peak stress–strain curve corresponding to the vertical direction, as shown in Fig. 13, cannot represent the real peak strength and the real softening response.

3.2.2. Friction angles

The friction angle is calculated from $\sin\phi = (\sigma_1 - \sigma_3)(\sigma_1 + \sigma_3)$, and Fig. 14 shows that it increases continuously with increasing b-value until $b = 0.15$. It then remains essentially constant as b increases in the

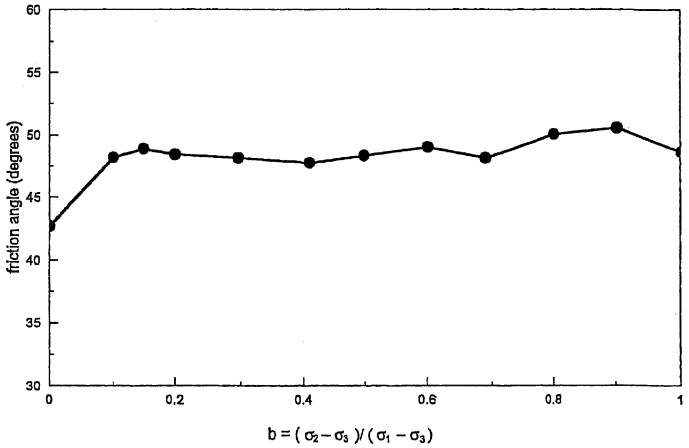

Fig. 14. Variation in friction angle with b-value for true triaxial tests on prismatic specimens of dense Santa Monica Beach sand with $\sigma'_3 = 49$ kPa.

range from 0.15 to 0.70. The friction angle increases slightly at $b = 0.90$, and then decreases slightly to $b = 1.0$. The lowest friction angle is obtained at $b = 0$ and the highest friction angle is reached at $b = 0.90$.

3.3. Conditions for shear banding

Bifurcation, i.e. initiation of shear band formation, is the inevitable result of continued shearing under conditions of uniform stresses and uniform strains: at some point, stress and strain states are reached which allow a localized displacement field to satisfy equilibrium, compatibility, boundary conditions, and constitutive relations (Rudnicki and Rice, 1975; Rice, 1976). This analysis procedure has been applied to study the influence of the constitutive model on the predicted shear banding (e.g. Molenkamp, 1985) and to investigate the conditions for shear banding under different three-dimensional stress conditions (e.g. Rudnicki and Rice, 1975; Vermeer, 1982; Peters et al., 1988; Peric et al., 1992).

The results of bifurcation analyses for three-dimensional stress and strain states are a set of critical plastic hardening moduli, H_c, which, when normalized on the elastic Young's modulus, E, vary with the value of b as indicated schematically in Fig. 15. A stress–strain state with a hardening modulus less than the critical hardening modulus can possibly produce shear banding.

The normalized, critical hardening modulus, H_c/E, at the point immediately before onset of shear banding, has been computed for each of the true triaxial tests on tall prismatic specimens of dense, medium dense, and loose sand. In this manner, the experimentally determined conditions for shear band formation under three-dimensional stress conditions can be established, and the pattern may be compared with the that shown in Fig. 15. The analysis required for this computation was presented by Lade and Wang (2001).

Fig. 16 shows the variation with b-value of H_c/E calculated immediately before onset of shear banding. The range of b giving positive H_c/E is about 0.18–0.85. Negative values of H_c/E are obtained for b in the ranges 0.0–0.18 and 0.85–1.0. The calculations for $b = 1.0$ are questionable, because failure in the cross-anisotropic sand specimen occurred in the load-controlled horizontal stress direction and the real peak point and post-peak stress–strain relation are not available. The variation of H_c/E in the mid-range and for high b-values compares well with that indicated by Rudnicki and Rice (1975) and shown in Fig. 15, and the calculated magnitudes compare well with those given by Peters et al. (1988) for medium and high b-values. However, the negative H_c/E-values obtained for small b-values are much smaller than those indicated by these authors. The calculations of critical hardening moduli were found to be rather sensitive to the actually measured slope of the stress–strain curves for low and high b-values, while they were more steady in the

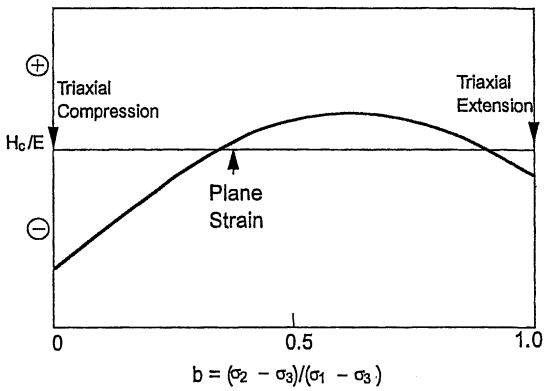

Fig. 15. Schematic diagram of variation of normalized, critical hardening modulus with b according to Rudnicki and Rice (1975) and Rice (1976).

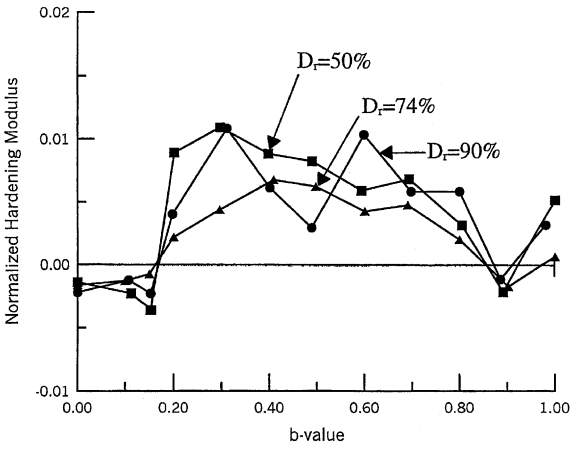

Fig. 16. Variation of normalized, critical hardening modulus, H_c/E with b for true triaxial tests on prismatic specimens of dense, medium dense, and loose Santa Monica Beach sand with $\sigma_3' = 49$ kPa.

mid-range of b-values where shear banding occurred in the hardening regime. According to the experimental evidence, shear banding causes failure in all experiments with $0.18 < b < 0.85$, although it occurs rather close to smooth peak failure for the tests with high b-values.

It can be concluded that the condition for shear band formation in a test with b in the range of 0.18–0.85 may be fulfilled in the hardening portion of the stress–strain curve, and the maximum strength which the specimen could produce under homogeneous conditions will therefore not be reached. The greater the value of the critical hardening modulus, the earlier the shear banding occurs before smooth peak failure. That is why very limited variations of strength and strain-to-failure were obtained for b in this range. However, for triaxial compression tests and tests at low b-values ($b < 0.18$) and at high b-values ($b > 0.85$), shear banding occurs in the softening regime.

3.4. Comparison of strengths with three-dimensional failure criteria

The strengths from the true triaxial tests on tall prismatic specimens of dense sand are compared in Fig. 17 with those predicted by Lade's failure criterion (1977) at $\sigma_3' = 49$ kPa. The failure criterion is fitted to the results of triaxial compression tests performed on short, cylindrical specimens, for which a complete set of data for several confining pressures were available. This type of test with height-to-diameter of unity typically produce slightly higher strengths than the tests on tall specimens, as also indicated in Fig. 17. For $b < 0.18$ and $b > 0.85$, the peak strengths are not influenced by shear banding and the experimentally determined strengths compare fairly well with the model predictions. However, this failure criterion does not capture the variation of strength for $0.18 < b < 0.85$. The strengths in this range cannot be fully mobilized due to the influence of shear banding in the hardening regime. This implies that a smooth, continuous three-dimensional failure surface generally is not be obtained for soils.

The failure points from the experiments on dense Santa Monica Beach sand are compared with Lade's failure surface and the Mohr–Coulomb failure surface in the octahedral plane in Fig. 18. It can be seen that while the Mohr–Coulomb criterion always underestimates the three-dimensional strengths produced at b greater than zero, Lade's failure criterion models the strengths with fairly good accuracy, except in the mid-range of b-values in which shear banding occurs in the hardening regime.

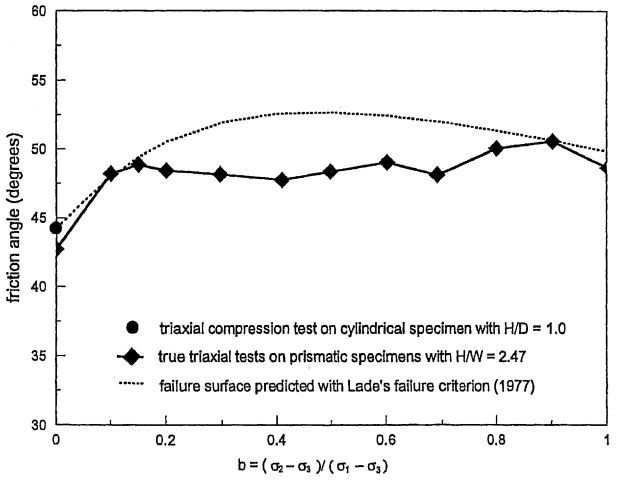

Fig. 17. Comparison Lade's failure surface with measured friction angles for true triaxial tests on prismatic specimens of dense Santa Monica Beach sand with $\sigma_3' = 49$ kPa. Effect of shear banding indicated in middle range of b-values.

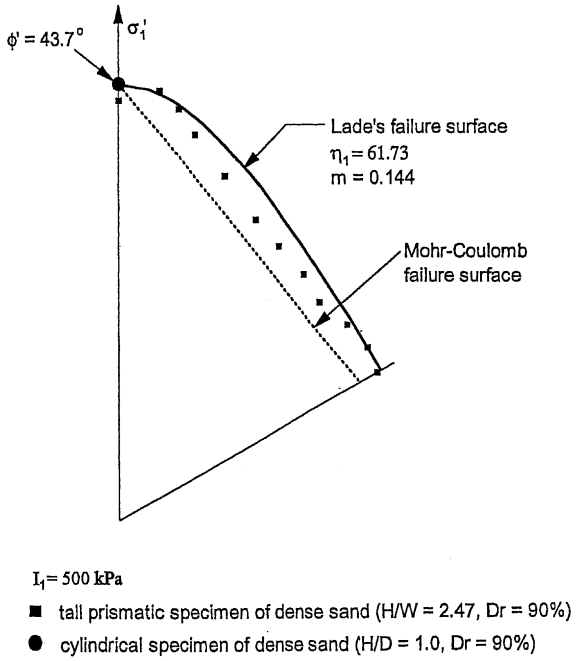

Fig. 18. Experimental failure surface for true triaxial tests on prismatic specimens of dense Santa Monica Beach sand with $\sigma_3' = 49$ kPa compared with the Mohr–Coulomb failure surface and Lade's failure surface.

4. Summary and conclusions

With background in the stability conditions proposed by Drucker and Hill, the stability of granular materials which exhibit nonassociated flow has been investigated on the basis of experimental observations.

Triaxial compression tests designed to expose the type of behavior exhibited by granular materials were performed. The variables in these studies were the sign of the second work increment (positive or negative), the volumetric strain behavior (compression or dilation), the constraints of the volumetric behavior (free or controlled), and the degree of saturation (fully or partly saturated). It is shown that the conditions for stability proposed by Drucker and by Hill are not necessary to guarantee stability of granular (frictional) materials. However, when these criteria are violated, it is possible to create an unstable situation by prescribing a constraint among the kinematic degrees of freedom (e.g. shear and volumetric strain). Conditions for stability are indicated on the basis of experimental observations of the behavior of granular materials in triaxial tests. The occurrence of instability involves small strains, and once it has been initiated it may lead to liquefaction which requires large strains to fully develop.

Shear planes occur in granular materials that dilate. In triaxial compression they develop after peak failure. The type of instability that manifests itself by shear plane development appears to be different from the instability relating to a decrease in load carrying capability occurring *inside* the failure surface for granular materials that contract during shear.

Shear banding, detected through the sudden strength reduction, initiates in the hardening regime of true triaxial tests when $b = (\sigma_2 - \sigma_3)/(\sigma_1 - \sigma_3)$ is in the approximate range of 0.18–0.85. Failure in these tests is considered to be a consequence of shear banding rather than a constitutive response. To verify this, the condition for shear band formation was examined for each test through the computation of the hardening modulus prior to onset of shear banding. For b-values in the ranges from 0 to 0.18 and from 0.85 to 1.0, negative hardening moduli were obtained, implying that conditions for shear band formation are fulfilled in the softening regime. Therefore, failure occurs by smooth peak failure and as a continuum response in these ranges. Positive values of the hardening modulus immediately before onset of shear banding was obtained when b was in the approximate range of 0.18–0.85, indicating that the condition for bifurcation is fulfilled in the hardening portion of stress–strain curve. Thus, peak failure is caused by shear banding in this middle range of b-values, and a smooth, continuous three-dimensional failure surface is therefore not obtained in general for soils.

References

Arthur, J.R.F., Dunstan, T., 1982. Rupture layers in granular media. In: Proceedings, IUTAM Symposium on Deformation and Failure of Granular Materials, Delft. Balkema, Rotterdam, pp. 453–459.

Arthur, J.R.F., Dunstan, T., Al-Ani, Q.A.J.L., Assadi, A., 1977. Plastic deformation and failure in granular media. Geotechnique 27 (1), 53–74.

Bishop, J.F.W., Hill, R., 1951. A theory of the plastic distortion of a polycrystalline aggregate under combined stresses. Philos. J. 42, 414–427.

Bjerrum, L., Simons, N.E., 1960. Comparison of shear strength characteristics of normally consolidated clays. In: Proceedings of the ASCE Research Conference. Boulder, Colorado, pp. 711–726.

Desrues, J., Chambon, R., Mokni, M., Mazerolle, F., 1996. Void ratio evolution inside shear bands in triaxial sand specimens studied by computed tomography. Geotechnique 46 (3), 529–546.

Desrues, J., Lanier, J., Stutz, P., 1985. Localization of the deformation in tests on sand sample. Eng. Fract. Mech. 21 (4), 909–921.

Drucker, D.C., 1951. A more fundamental approach to stress–strain relations. In: Proceedings of the First US Nat. Cong. Appl. Mech., pp. 487–491.

Drucker, D.C., 1956. On uniqueness in the theory of plasticity. Quart. Appl. Math. 14, 35–42.

Drucker, D.C., 1959. A definition of stable inelastic material. J. Appl. Mech. 26, 101–106.

Finno, R.J., Harris, W.W., Mooney, M.A., Viggiani, G., 1996. Strain localization and undrained steady state of sand. J. Geotech. Eng. 122 (6), 462–473.

Finno, R.J., Harris, W.W., Mooney, M.A., Viggiani, G., 1997. Shear bands in plane strain compression of loose sand. Geotechnique 47 (1), 149–165.

Hettler, A., Vardoulakis, I., 1984. Behavior of dry sand tested in a large triaxial apparatus. Geotechnique 34, 183–197.

Hill, R., 1958. A general theory of uniqueness and stability in elastic–plastic solids. J. Mech. Phys. Solids 6, 236–249.

Lade, P.V., 1977. Elasto-plastic stress–strain theory for cohesionless soil with curved yield surfaces. Int. J. Solids Struct. 13, 1019–1035.
Lade, P.V., 1982. Localization effects in triaxial tests on sand. In: Proceedings, IUTAM Symposium on Deformation and Failure of Granular Materials, Delft, pp. 461–471.
Lade, P.V., 1989. Instability and failure of soils with nonassociated flow. In: Proceedings of the Twelvth International Conference on Soil Mech. Found. Eng., vol. 1. Rio de Janeiro, Brazil, pp. 727–730.
Lade, P.V., Bopp, P.A., Peters, J.F., 1993. Instability of dilating sand. In: Mechanics of Materials, vol. 16. Elsevier Science Publishers, pp. 249–264.
Lade, P.V., Duncan, J.M., 1973. Cubical triaxial tests on cohesionless soils. ASCE J. Soil Mech. Found. Div. 99 (SM10), 793–812.
Lade, P.V., Duncan, J.M., 1976. Stress-path dependent behavior of cohesionless soil. J. Geot. Eng. Div., ASCE 102, 51–68.
Lade, P.V., Nelson, R.B., Ito, Y.M., 1987. Nonassociated flow and stability of granular materials. ASCE J. Eng. Mech. 113, 1302–1318.
Lade, P.V., Nelson, R.B., Ito, Y.M., 1988. Instability of granular materials with nonassociated flow. ASCE J. Eng. Mech. 114, 2173–2191.
Lade, P.V., Pradel, D., 1990. Instability and flow of granular materials. I: experimental observations. ASCE J. Eng. Mech. 116, 2532–2550.
Lade, P.V., Wang, Q., 2001. Analysis of shear banding in true triaxial tests on sand. ASCE J. Eng. Mech. 127, 762–768.
Mandel, J., 1964. Conditions de stabilite et postulat de Drucker. In: Proceedings, IUTAM Symposium on Rheology and Soil Mechanics Grenoble, pp. 58–68.
Molenkamp, F., 1985. Comparison of frictional material models with respect to shear band initiation. Geotechnique 35, 127–143.
Mroz, Z., 1963. Nonassociated flow laws in plasticity. J. de Mecanique 2, 21–42.
Nemat-Nasser, S., 1983. On finite plastic flow of crystalline solids and geomaterials. J. Appl. Mech. 105, 1114–1126.
Peric, D., Runesson, K., Sture, S., 1992. Evaluation of plastic bifurcation for plane strain versus axisymmetry. ASCE J. Eng. Mech. 118 (3), 512–524.
Peters, J.F., 1991. Discussion of instability of granular materials with nonassociated flow. ASCE J. Eng. Mech. 117, 934–936.
Peters, J.F., Lade, P.V., Bro, A., 1988. Shear band formation in triaxial and plane strain tests. In: Advanced Triaxial Testing of Soil and Rock, vol. 977. ASTM STP, pp. 604–627.
Poorooshasb, H.B., Holubec, I., Sherbourne, A.N., 1966. Yielding and flow of sand in triaxial compression: Part I. Can. Geot. J. 3, 179–190.
Rice, J.R., 1976. The localization of plastic deformation. In: Koiter, W.T. (Ed.), Proceedings of the Fourth Conf. on Theoret. and Appl. Mech. North-Holland Publishing Co., Amsterdam, pp. 207–229.
Rudnicki, J.W., Rice, J.R., 1975. Conditions for the localization of deformation in pressure-sensitive dilatant materials. J. Mech. Phys. Solids 23, 371–394.
Seed, H.B., Mitchell, J.K., Chan, C.K., 1960. The strength of compacted cohesive soils. In: Proceedings of the ASCE Research Conference. Boulder, Colorado, pp. 877–964.
Vardoulakis, I., 1980. Shear band inclination and shear modulus of sand in biaxial tests. Int. J. Numer. Anal. Meth. Geomech. 4, 103–119.
Vermeer, P.A., 1982. A simple shear-band analysis using compliances. In: IUTAM Conference on Deformation and Failure of Granular Materials, Delft, pp. 493–499.
Wang, Q., Lade, P.V., 2001. Shear banding in true triaxial tests and its effect on failure in sand. ASCE J. Eng. Mech. 127, 754–761.
Whitman, R.V., 1960. Some considerations and data regarding the shear strength of clays. In: Proceedings of the ASCE Research Conference. Boulder, Colorado, pp. 581–614.
Yoshida, T., Tatsuoka, F., Siddiquee, M.S.A., Kamegai, Y., Park, C.-S., 1993. Shear banding in sands observed in plane strain compression. In: Proceedings of the Third International Workshop Localisation and Bifurcation Theory for Soils and Rocks. Grenoble, pp. 165–179.